NeuroImage 294 (2024) 120647

Contents lists available at ScienceDirect

NeuroImage

journal homepage: www.elsevier.com/locate/ynimg

# Non-invasive electrical brain stimulation modulates human conscious perception of mental representation

Jeehye Seo [a,b], Byoung-Kyong Min [a,b,c,*]

[a] Institute of Brain and Cognitive Engineering, Korea University, Seoul 02841, South Korea
[b] BK21 Four Institute of Precision Public Health, Korea University, Seoul 02841, South Korea
[c] Department of Brain and Cognitive Engineering, Korea University, Seoul 02841, South Korea

ARTICLE INFO

*Keywords:*
Conscious perception
Functional magnetic resonance imaging
Higher-order thalamocortical network
Mental representation
Non-invasive electrical brain stimulation
Transcranial alternating current stimulation

ABSTRACT

Mental representation is a key concept in cognitive science; nevertheless, its neural foundations remain elusive. We employed non-invasive electrical brain stimulation and functional magnetic resonance imaging to address this. During this process, participants perceived flickering red and green visual stimuli, discerning them either as distinct, non-fused colours or as a mentally generated, fused colour (orange). The application of transcranial alternating current stimulation to the medial prefrontal region (a key node of the default-mode network) suppressed haemodynamic activation in higher-order subthalamic and central executive networks associated with the perception of fused colours. This implies that higher-order thalamocortical and default-mode networks are crucial in humans' conscious perception of mental representation.

## 1. Introduction

The experience of conscious perception of mental representations is fundamental to everyday life; however, the neural correlates underlying this process remain unclear. To systematically investigate this, we conducted a visual flickering experiment to examine the role of thalamocortical interactions in the conscious perception of mental representation using magnetoencephalography (MEG) (Min et al., 2020) and functional magnetic resonance imaging (fMRI) (Seo et al., 2022). In comparing physically existing individual red/green colours with their illusory fused orange colour, we observed thalamocortical inhibitory coupling between the thalamus and visual cortex during conscious perception. A series of our previous studies provides theoretical (Min, 2010) and empirical (Min et al., 2020; Seo et al., 2022) evidence that the thalamocortical inhibitory network is a gateway to conscious mental representations. In addition to our previous neuroimaging studies, the present study aimed to actively perturbate conscious perception of mental representations using non-invasive electrical brain stimulation, thereby providing neuromodulatory evidence for the pivotal role of the thalamocortical inhibitory network in human conscious perception.

The conscious perception of mental representations has been suggested to involve iterative and integrative communication across modal-specific individual thalamic subdivisions and their corresponding cortices (Min, 2010). Thalamic relay nuclei can be broadly categorised into first-order and higher-order thalamic relay nuclei (Sherman, 2016). For instance, the lateral geniculate nucleus (LGN) and pulvinar represent first- and higher-order thalamic relay cells involved in visual processing, respectively. Conscious perception becomes more refined as higher-order relay signals run cumulatively through relevant thalamocortical loops. Additionally, the coordination between the mutually antagonistic central-executive network (CEN) and default-mode network (DMN) is acknowledged to regulate neural responses underlying fundamental brain functions (Nekovarova et al., 2014). The switching dynamics between these two networks are controlled by the salience network (SN), which recruits relevant functional networks (Menon and Uddin, 2010; Peters et al., 2016; Sridharan et al., 2008). In our study, we applied transcranial alternating current stimulation (tACS) to representative nodes of the mutually antagonistic networks (dorsolateral prefrontal cortex [DLPFC] for the CEN and medial prefrontal cortex [mPFC] for the DMN), with tACS to V1 serving as a control for the lower hierarchy of the visual processing stage. We selected 12 regions of interest (ROIs) to explore task-relevant thalamocortical neurodynamics (using fMRI beta weights), encompassing significantly activated regions during the task and crucial areas for the CEN, DMN,

* Corresponding author at: Department of Brain and Cognitive Engineering, Director, Institute of Brain and Cognitive Engineering, Korea University, Seoul 02841, South Korea.
*E-mail address:* min_bk@korea.ac.kr (B.-K. Min).

https://doi.org/10.1016/j.neuroimage.2024.120647
Received 28 February 2024; Received in revised form 9 May 2024; Accepted 13 May 2024

and SN: LGN, pulvinar, medial dorsal nucleus of the thalamus (MD), V1, V2, V4, posterior cingulate cortex (PCC), anterior insular cortex (AIC), dorsal anterior cingulate cortex (dACC), posterior parietal cortex (PPC), mPFC, and DLPFC.

Utilising mental perception based on a physically non-existent substrate provides an optimal opportunity to investigate the neurophysiological foundations of conscious perception of mental representation. We explored the conscious perception of mental representations by employing an experimental paradigm that presented participants with two individual colours, red and green. When participants were exposed to these two colours in a rapidly alternating pattern, they occasionally perceived a novel colour—the fused orange. Consequently, under the same stimulation conditions, distinct conscious perceptions (fusion or non-fusion) were observed within the same individual. The stimuli were presented using a 5 × 5 array of bicolour (red and green) light-emitting diode (LED) lamps (Fig. S1). To ensure the reliability of the neuromodulatory outcomes in comparison to our prior observations in the MEG (Min et al., 2020) and fMRI (Seo et al., 2022) studies, we adopted the same experimental paradigm. Despite various presentation times explored in our previous MEG investigation (Min et al., 2020), the current tACS-fMRI study specifically employed the 50-ms flickering condition. This choice was based on the observation that the identical physical presentation of the 50-ms flickering condition occasionally elicited different perceptual responses of either the fusion or non-fusion condition. Therefore, conscious perception of the fused colour was solely influenced by subjective top-down processing rather than being driven by physically induced bottom-up processing.

## 2. Results

In the absence of tACS treatment, the 50 ms flickering condition showed no significant differences in responses between the fusion (47.8 %) and non-fusion (52.2 %) conditions ($t$ (21) = –0.408, *n.s.*). However, there was a significant interaction effect between the tACS target-region and perceptual factors on response rates ($F$ (3, 126) = 15.319, $p$ < 0.001). Subsequent tests revealed that tACS applied to mPFC resulted in significantly more fusion responses (77.3 %) than non-fusion responses (22.7 %; $t$ (21) = 5.541, false discovery rate [FDR]-corrected $p$ < 0.001). This substantial enhancement in the fusion response was also evident when tACS was applied to V1 ($t$ (21) = 3.435, FDR-corrected $p$ < 0.01; fusion, 73.3 %; non-fusion, 26.7 %) and when tACS was applied to DLPFC ($t$ (21) = 2.265, FDR-corrected $p$ = 0.051; fusion, 66.1 %; non-fusion, 33.9 %; Fig. 1).

We examined tACS-mediated functional activation of the fusion and non-fusion conditions using the standard general linear model (GLM) pipeline of SPM12 (https://www.fil.ion.ucl.ac.uk/spm/software/spm12). The contrasts of interest encompassed 'fusion – fixation', 'non-fusion – fixation', and 'fusion – non-fusion'. Precisely, 'fusion – fixation' and 'non-fusion – fixation' represented within-condition contrasts, and their difference (fusion minus non-fusion) constituted the between-condition contrast during 50-ms flickering stimulation. The fixation condition was defined based on the interval between the participant's response onset and the subsequent flickering onset (mean ± SD: 7.16 ± 0.37 s). The visual cortices, including the V2, cuneus, and fusiform regions, exhibited greater activation in the non-fusion condition compared to the fusion condition without tACS treatment (Fig. 2A). Notably, tACS applied to the mPFC led to significantly suppressed activation in the fusion condition versus the non-fusion condition, particularly in higher-order subthalamic regions such as the pulvinar and medial dorsal nucleus of the thalamus (MD), and the CEN (DLPFC and PPC), the DMN (precuneus), and the SN (AIC; Fig. 2B). There were no significant differences in deactivation between the fusion and non-fusion conditions for the no-tACS or tACS-to-mPFC conditions. TACS applied to the V1 and DLPFC did not result in any significant haemodynamic changes (activation or deactivation) between the fusion and non-fusion conditions. Table S1 displays the Montreal Neurological Institute (MNI) coordinates of significantly activated brain regions for differences between fusion and non-fusion responses, depending on the tACS treatment condition.

As illustrated in the temporal dynamic changes of fMRI beta weights (Fig. 3), compared with the no-tACS treatment, it was consistently shown that the tACS-to-mPFC demonstrated significant suppression of haemodynamics in higher-order thalamocortical regions, including the pulvinar, V4, DLPFC, PPC, and AIC, for the fusion condition compared with the non-fusion condition (highlighted by red boxes in Fig. 3B). Simultaneously, relative to the no-tACS treatment, tACS-to-mPFC significantly suppressed activation in the pulvinar, V4, DLPFC, and AIC under fusion conditions (indicated by orange asterisks in Fig. 3B), while enhancing activation in the mPFC under fusion conditions (orange asterisks in Fig. 3B) and V1 under non-fusion conditions (blue asterisks in Fig. 3B). However, the tACS-to-DLPFC condition did not exhibit significant tACS-mediated differences between fusion and non-fusion responses (Fig. 3C). In contrast, compared with the substantial influence on the activation difference between fusion and non-fusion perception by the tACS-to-mPFC, tACS-to-V1 induced suppression of activation only in higher-order cortices such as the DLPFC, PPC, AIC, and dACC in the fusion condition compared with the non-fusion condition (highlighted by red boxes in Fig. 3A). Compared to the no-tACS treatment, the tACS-to-V1 treatment resulted in significant suppression of activation in the LGN, V4, AIC, and DLPFC in the fusion condition (orange asterisks in Fig. 3A) and significant suppression of activation in V4 and DLPFC in the non-fusion condition (blue asterisks in Fig. 3A).

## 3. Discussion

This non-invasive neuromodulatory study aimed to provide

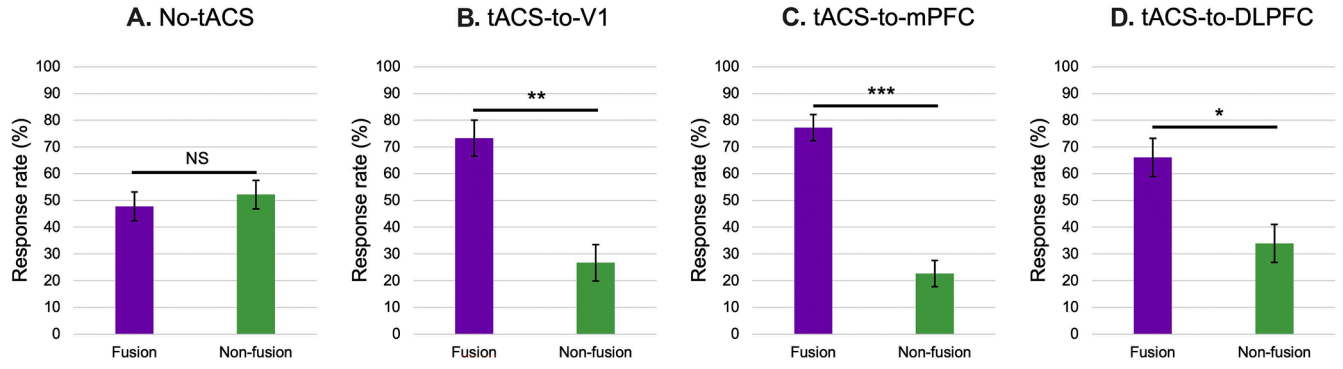


**Fig. 1.** tACS-mediated changes in response rates. Response rates (%) to the fusion (orange) and non-fusion (red/green) perception in the (A) no-tACS, (B) tACS to V1, (C) tACS to mPFC, and (D) tACS to DLPFC treatments. Error bars indicate standard errors of the mean; $N$ = 22, FDR-corrected * $p$ = 0.051; ** $p$ < 0.01; *** $p$ < 0.001; *NS*, non-significant; paired sample $t$-test.

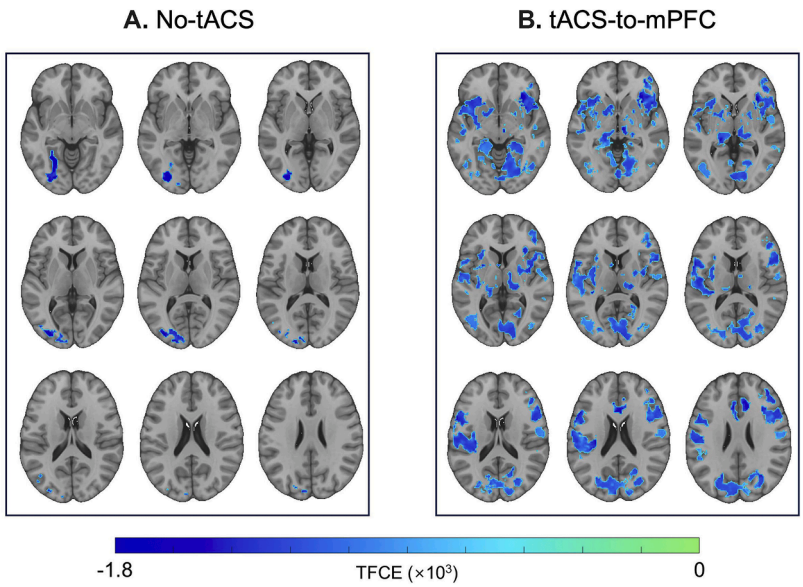


**Fig. 2.** tACS-mediated functional activation during the visual perception task. Functional activation differences between fusion and non-fusion perception under the (A) no-tACS and (B) tACS-to-mPFC treatment are displayed using the between-condition contrast from a random-effects GLM (threshold-free cluster enhancement [TFCE] family-wise error rate [FWE]-corrected $p < 0.05$, $k \geq 100$). Note that thalamocortical activation during the tACS-to-mPFC condition was compared with the no-tACS treatment, where blue colour represents decreased task activity during visual perception processing. In activation difference (fusion – non-fusion perception), the fusion condition showed suppressed activation in the higher-order subthalamic regions (pulvinar and MD), the CEN (DLPFC and PPC), the DMN (precuneus), and the SN (AIC; blue clusters, TFCE FWE-corrected $p < 0.05$, $k \geq 100$). Axial slices are evenly spread from $z = -6$ to $z = 26$ in the MNI 152 template. *Abbreviations:* CEN, central executive network; DMN, default mode network; SN, salience network; mPFC, medial prefrontal cortex; PPC, posterior parietal cortex; DLPFC, dorsolateral prefrontal cortex; AIC, anterior insular cortex; MD, medial dorsal nucleus of the thalamus.

haemodynamic evidence supporting the crucial role of thalamic inhibitory regulation during conscious perception of mental representations in humans. Notably, the tACS-to-mPFC condition demonstrated that the primary (first-order) thalamic region, such as the LGN, exhibited no significant differences between the fusion and non-fusion conditions. However, the pulvinar (belonging to the higher-order visual thalamic nuclei) showed significant differences under the tACS-to-mPFC treatment (Fig. 3B). For higher-order visual cortical regions, including the V4, AIC, PPC, and DLPFC, significant tACS-mediated differences between the fusion and non-fusion conditions were observed, in contrast to almost no significant differences in lower-order visual cortical regions (V1 and V2).

The present tACS-applied fMRI observations, in conjunction with findings from our previous MEG (Min et al., 2020) and fMRI (Seo et al., 2022) investigations, collectively provide supporting evidence for the crucial role of higher-order thalamocortical inhibitory control and integrative signal communications across the thalamocortical networks of the CEN, DMN, and SN in conscious perception, distinguishing between fusion (illusory) and non-fusion mental representations. When compared with tACS conditions applied to other regions such as V1 and DLPFC, tACS to the mPFC (a key node of the DMN) led to significantly suppressed activation in higher-order thalamic cells (pulvinar and MD), SN (AI), DMN (precuneus), and CEN (DLPFC and PPC) during fused colour perception compared to non-fused colour perception (Fig. 2B). These observations were consistently supported by subsequent analyses of temporally sequential neurodynamic trajectories (Fig. 3B). Although the tACS-to-DLPFC did not exhibit significant differences between fused and non-fused colour perception, it sometimes yielded significant changes in fMRI beta weights compared to the no-tACS condition (see the pulvinar, V4, AIC, mPFC, and DLPFC in Fig. 3). Presumably, depending on the target region for tACS, tACS intervention was involved in different stages of visual information processing within multiple levels of the visual processing hierarchy. For example, tACS-to-V1 might intervene in the early stage of visual processing, whereas tACS-to-DLPFC might mediate the late stage of decision-making, all of which could contribute to significant alterations in the perception of fused colour. However, the mPFC appears to be the optimal location where both tACS-mediated behavioural and haemodynamic changes are induced when stimulated.

Within this framework, our findings reinforce the pivotal role of the DMN in the conscious perception of internal mental representation, specifically the illusory-fused colour perception. This aligns with our previous fMRI study (Seo et al., 2022). Notably, in contrast to non-significant haemodynamic differences between fusion and non-fusion conditions under tACS applied to DLPFC (a key node of CEN), tACS to mPFC (a key node of DMN) resulted in significantly suppressed haemodynamic activation of the CEN, DMN, and SN during fusion perception (subjective imagery experience) compared to non-fusion perception (highlighted by red boxes in Fig. 3B). As the tACS-mediated functional perturbation of the DMN node modulated the conscious perception of mental representation, the DMN, but not CEN, appears to play a pivotal role in the mental representation of illusory (fused) colour perception. The essential role of the DMN as a modality-independent core mental imagery network has been consistently reported (Daselaar et al., 2010; Zhang et al., 2018b). Visual illusions have been suggested to involve increased engagement of the DMN with the primary visual system (Shine et al., 2015). The significance of the DMN has been associated with building and updating internal world models during conscious perception (Ramírez-Barrantes et al., 2019). Ongoing conscious experience has been consistently studied concerning the DMN (Smallwood et al., 2021; Sormaz et al., 2018; Stawarczyk et al., 2011). There appears to be an association between the formation of the internal representation of a mentally fused colour and pronounced changes in DMN activity compared with the perception of physically existing colours, red and green. This DMN-based mental representation may be informative regarding the identity of human consciousness because conscious perception of mental representation can be achieved without external or physical stimulation.

Furthermore, the AIC exhibited significantly different tACS-mediated neurodynamics between the fusion and non-fusion

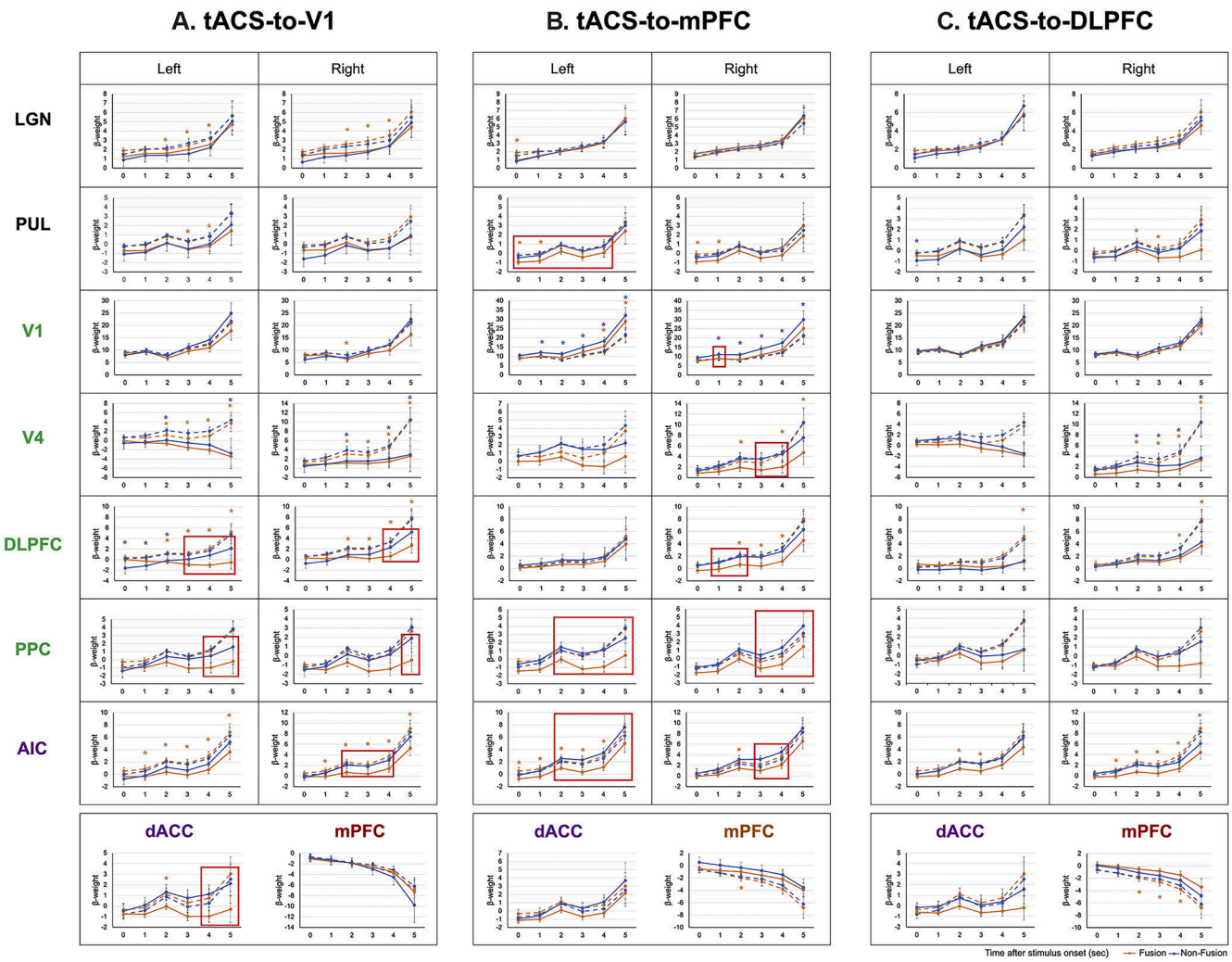


**Fig. 3.** tACS-mediated temporal dynamics of regional brain activity. Temporal dynamic changes of fMRI beta weights between the fusion (orange curves) and non-fusion (blue curves) conditions in 9 ROIs of left and right hemispheres, as a function of time after visual stimulus onset during (A) tACS to V1, (B) tACS to mPFC, and (C) tACS to DLPFC. Dashed lines indicate the no-tACS treatment. Since the other 3 ROIs (i.e., MD, V2, and PCC) did not show tACS-mediated significant differences between fusion and non-fusion responses, they are not shown here. Beta weights were computed from the GLM of their blood-oxygen-level-dependent (BOLD) signals. The red boxes indicate statistical significance (false discovery rate [FDR]-corrected $p < 0.05$) between fusion and non-fusion conditions in the tACS treatment. Asterisks represent statistical significance (FDR-corrected $p < 0.05$) of tACS-mediated changes relative to no-tACS treatment (orange asterisks for the fusion condition and blue ones for the non-fusion condition). Error bars indicate standard errors of the mean. *Abbreviations:* AIC, anterior insular cortex; dACC, dorsal anterior cingulate cortex; DLPFC, dorsolateral prefrontal cortex; LGN, lateral geniculate nucleus; mPFC, medial prefrontal cortex; PPC, posterior parietal cortex; PUL, pulvinar; V1, primary visual cortex; V4. Different font colours of ROIs are used for thalamic regions (black), CEN regions (green), SN regions (purple), and DMN regions (brown).

conditions (Fig. 3). Crucially, core DMN regions are known to be anti-correlated with the dorsal AIC (dAIC) and dACC (Chang and Glover, 2009; Fox et al., 2005), forming a functional connection with regions associated with a cognitive control and decision-making network (Dosenbach et al., 2007; Grinband et al., 2006). The insula, recognised as a multimodal integration region, serves as an interface between external information and internal motivational states (Craig, 2009; Seeley et al., 2007). Differentiating from the posterior insula, the anti-correlation pattern between the DMN and CEN is modulated by an AIC-based network, primarily composed of the AIC and dACC (Chand and Dhamala, 2016; Sridharan et al., 2008), being associated with neural correlates of consciousness (Craig, 2009; Zhang et al., 2018a). The AIC, involved in various cognitive processes such as switching between cognitive resources (Uddin and Menon, 2009) and reorienting attention (Ullsperger et al., 2010), consistently appears to be implicated in switching the dominant processing network between the CEN and DMN in this study. Furthermore, the temporal haemodynamics of dACC were further modulated by tACS-to-V1 than tACS-to-mPFC (Fig. 3A), suggesting a stronger functional association between dACC and V1 than mPFC during mental imagery.

Notably, the tACS-to-mPFC condition induced significantly suppressed activation in the pulvinar for the fusion condition compared to the non-fusion condition. As the pulvinar plays a thalamic role in advanced visual information processing (Arcaro et al., 2015; Barron et al., 2015), refined visual signals in the pulvinar may propagate to higher-order visual processing cortices, including the V4, PPC, and DLPFC. This observation implies substantial involvement of higher-order thalamic disinhibition during conscious perception of the mentally fused illusory orange colour. As the thalamic reticular nucleus (TRN) primarily contributes to the inhibitory feedback control of thalamocortical neurons (Lopes da Silva, 1991; Shu and McCormick, 2002), these observations consistently support the TRN-mediated thalamocortical inhibitory control model for the conscious perception of mental representation (Min, 2010). Throughout the latticework structure of the

TRN, conscious perception could be established and refined through accumulating intercommunicative processing across first-order input and higher-order signals over relevant thalamocortical loops. This supports the TRN-centred thalamocortical inhibitory networking model of conscious perception in humans (Min, 2010).

However, this study has several limitations. First, although a larger sample size would have improved the statistical power of our study, the sample sizes were limited by multiple tACS target groupings (i.e., tACS-to-V1, tACS-to-mPFC, and tACS-to-DLPFC). Additionally, based on the current observations in healthy individuals, although it is difficult to figure out the expected result using a more diverse participant pool, further compelling evidence will be expected when recruiting participants with neurological or psychiatric impairments. For instance, patients with impairments in the mPFC may exhibit potential biases toward either fused or non-fused colour perception when tACS-to-mPFC is administered. Second, although we used an MR-compatible tACS system and compared two perceptual (or stimulation) conditions that are commonly associated with potential tACS-induced artefacts or influences on fMRI signals (or MR-induced alterations on tACS), these potential mutually confounding interferences (Alekseichuk et al., 2016; Antal et al., 2014; Vosskuhl et al., 2016) should be considered when interpreting the current observations. Third, we interpreted the present observations as implying substantial involvement of higher-order thalamic disinhibition during conscious perception of the mentally fused illusory orange colour. This is because the pulvinar and medial dorsal nucleus of the thalamus (both higher-order subthalamic nuclei) showed significantly suppressed activation for the perception of the fused colour; however, more direct empirical evidence is necessary for this argument. In future studies, non-invasive stimulation specifically focusing on the thalamus using focused ultrasound (Legon et al., 2018) or tACS with a temporal-interference technique (Grossman et al., 2017) will provide further convincing evidence supporting the involvement of thalamocortical networks during conscious perception of fused colours.

In summary, based on the coupled thalamocortical haemodynamics examined in this study, the higher-order subthalamic regions and DMN appear to be crucial neural signatures of mental representation within the entire CEN and SN systems of thalamocortical loops, serving as a dynamic core in conscious experience. Our present neuromodulation study, together with previous MEG (Min et al., 2020) and fMRI (Seo et al., 2022) studies, provides corroborating support for the importance of thalamocortical inhibitory control in human conscious perception of mental representation, acknowledging the current limitations of human neuroimaging and non-invasive neuromodulatory techniques. Since the sustainability or long-term effects of tACS (Kasten et al., 2016; Kasten and Herrmann, 2022) is also crucial in a neuromodulatory approach, future studies should focus on the carrier-over or wash-out effect using this tACS-mediated perceptual paradigm.

## 4. Materials and methods

### 4.1. Participants

Thirty-five healthy volunteers (age: 24.8 ± 2.9 years; 20 men and 15 women) participated in the study. All participants had normal or corrected-to-normal vision and passed the Ishihara colour test, confirming that none were colour-blind. All participants were free of neurological and psychiatric illnesses, contra-indications for magnetic resonance imaging (MRI), current and past alcohol/drug abuse or dependence, and current use of illicit substances. All participants provided written informed consent and received compensation for their participation. The study adhered to ethical guidelines set by the Institutional Review Board of Korea University (No. KUIRB-2021–0209–08) and the Declaration of Helsinki (World Medical Association, 2013).

### 4.2. Materials and procedure

Stimuli were presented in a 5 × 5 array of 3-mm round diffused bicolour (red and green) light-emitting diode (LED) lamps (model number: 100F3W-YT-REGR-CA, Chanzon Technology) (Min et al., 2020). Five rows and columns of the LED grid were lit on a black panel with a 1-cm gap between two adjacent rows or columns (Fig. S1). Red light had 620–625 nm wavelengths, while green light had 515–520 nm wavelengths. These wavelengths are relevant for stimulating human retinal long-wave and middle-wave photoreceptors exhibiting optimal responses to the colours, as their mean absorbance wavelengths are 562.8 nm and 533.8 nm for red and green, respectively (Bowmaker and Dartnall, 1980). According to the CIE 1931 RGB colour-matching function (CIE, 1931), the monochromatic test revealed maximal peaks at approximately 610 nm for red and 540 nm for green. To mitigate potential confounding luminance effects, the luminous intensity was balanced across these two colours to the extent possible in psychometric and physical terms (approximately 800 mcd). A thin plastic diffuser covered the LED array to ensure even light distribution.

The experimental paradigm employed in this study draws from our previous MEG (Min et al., 2020) and fMRI (Seo et al., 2022) studies, investigating neurodynamic changes within the thalamocortical network. Among various presentation times utilised in our MEG (Min et al., 2020) study, the current neuromodulatory study adopted the 50-ms flickering condition. This choice was made because the same physical (bottom-up) stimulation of the 50-ms flickering stimuli occasionally resulted in different subjective perceptual (top-down) responses, either fusion or non-fusion. This condition proved optimal for exploring the top-down aspects of conscious perception. In the 50-ms presentation condition, red and green LEDs alternately flickered with a 50-ms individual flickering time, and these flickering colour stimuli were presented for 5 s in each trial, with variable intertrial intervals ranging from 6 s to 10 s (centred at 8 s). A 5-ms empty presentation gap was inserted between two consecutive red and green stimuli to prevent possible retinal afterimages. This gap may play a wash-out role in the previously presented colour stimulation on the retina, as the time courses of retinal afterimages are interrupted by the duration of the temporal gap (Di Lollo et al., 1988).

Participants underwent two experimental sessions, each involving two randomly assigned treatments among no-tACS, tACS-to-V1, tACS-to-mPFC, and tACS-to-DLPFC, with a minimum of 2-day separation between sessions. ‘No-tACS’ indicates a flickering-task performance without tACS treatment. The participants and the examiners who performed the tACS protocols were blinded to the type of stimulation. The experiment of each daily session included two runs of fMRI scanning (each for a different type of tACS treatment), with a short break in between. The order of tACS treatments was counterbalanced across participants. The colour flickering task was repeatedly applied to the same participants during each experimental run to investigate the impact of tACS treatment on colour perception performance. Thirty trials of the 50-ms flickering condition were randomly presented within each run. Participants were instructed to press a button with their right or left thumb based on whether they perceived a fused orange colour, with response hands counterbalanced across participants. To avoid movement artefacts, participants were instructed to press a button after the conclusion of each 5-s flickering presentation. Response rates were compared using repeated-measures ANOVA with a tACS target-region factor (no-tACS, tACS-to-V1, tACS-to-mPFC, and tACS-to-DLPFC) and a perceptual factor (fusion and non-fusion) of the tACS-mediated colour-flickering task. If a significant interaction effect was detected, subsequent tests were conducted using FDR-corrected two-sided paired *t*-tests (Benjamini and Hochberg, 1995).

In this study, the left/right V1 (primary visual cortex), mPFC (a key node of the DMN), and left/right DLPFC (a key node of the CEN) were chosen as the tACS target regions. As shown in Fig. S2A (sample channel montage), each target region comprised stimulation input electrodes

(marked in red) and surrounding return electrodes (marked in blue). All stimulation and return channels' currents were configured to maintain a total current of zero. Using the SimNIBS software (ver. 3.2.6, DRCMR & DTU, Denmark) (Thielscher et al., 2015) and tES LAB (ver. 3.0, Neurophet, Seoul, Korea) simulation software, we assessed whether the stimulation regions aligned well with the intended target regions before the main study (Fig. S2B). The average electric field intensity at the activated cortical region was 0.12 V/m.

Given that the 50-ms flickering frequency matched 9 Hz when consecutive inputs of two colours were considered a single perceptual unit (100 ms + 10 ms gap) and 18 Hz when each colour was considered a separate unit (50 ms + 5 ms gap), both frequencies were employed as tACS stimulation frequencies. Additionally, considering that EEG alpha activity is predominantly observed in the occipital region, and EEG beta activity is associated with top-down processing in the prefrontal region (Brincat and Miller, 2016; Miller et al., 2018; Min et al., 2021), 9 Hz (in the alpha band) was used for tACS-to-V1, and 18 Hz (in the beta band) was used for prefrontal tACS (tACS-to-DLPFC and tACS-to-mPFC). Although we used the occipital alpha frequency (9 Hz) and frontal beta frequency (18 Hz) for each tACS, the use of distinct frequencies (9 versus 18 Hz) *per se* may induce differences in brain activation patterns, which should be carefully considered when interpreting our observations.

The tACS was delivered online for the entire fMRI scanning duration (15 min 10 s) of the colour-flickering task using an MR-compatible $M \times N$ 65 high-definition (HD) transcranial electrical stimulator (tES) system (Soterix Medical Inc., New York, USA). TACS intensities were kept below individual sensation thresholds, and the peak-to-peak amplitude ranged from 0.2 to 1.5 mA, customised for each participant.

### 4.3. fMRI acquisition

MR images were acquired using a Siemens 3T MAGNETOM Trio Tim Syngo scanner (Siemens Healthcare, Erlangen, Germany) equipped with a 32-channel head coil. Before the experiment, participants received a detailed overview of the experimental procedure and were familiarised with the experimental environment and stimuli. They were instructed to keep their eyes open and focus on the LED panel outside the MRI shielding room through a mirror on the head coil. The LED light was visible through an electromagnetically shielded window, and the distance between the LED panel and the participants was approximately 520 cm, resulting in a visual angle of 0.8°. To optimise colour perception, the inside and outside of the MRI-shielding room were kept dark during the LED flickering experiment.

FMRI data were collected using an echo-planar image sequence with the removal of the first 5 vol (~10 s), resulting in a total of 455 vol (~15 min 10 s) [repetition time (TR) = 2 s; echo time (TE) = 30 ms; flip angle (FA) = 90°; multi-band acceleration factor = 3; acquisition matrix = 96 × 96; field of view (FOV) = 192 × 192 $mm^2$; in-plane voxel size = 2 × 2 × 2 $mm^3$; 75 transverse slices; no slice gap]. Three-dimensional anatomical magnetisation-prepared rapid gradient-echo (MP-RAGE) images were obtained for each participant following fMRI data collection [TR = 2.3 s; TE = 2.13 ms; inversion time (TI) = 0.9 s; FA = 9°, acquisition matrix = 256 × 256, in-plane voxel size = 1 × 1 × 1 $mm^3$, 224 sagittal slices].

### 4.4. fMRI pre-processing

Data pre-processing was conducted using SPM12 (https://www.fil.ion.ucl.ac.uk/spm/software/spm12). Standard task-based fMRI processing procedures were applied to functional scans, including slice-timing correction (using the first slice as the reference slice), motion correction, co-registration, grey/white matter segmentation, normalisation to the Montreal Neurological Institute (MNI) template, and spatial smoothing using a 6-mm full-width at half-maximum (FWHM) Gaussian kernel. To mitigate potential head-motion effects, participants with substantial motion were excluded based on the criteria: (1) average head movement, measured with frame-wise displacement (FD), exceeding 0.2 mm and (2) the percentage of volumes exhibiting high motion (defined as relative FD > 0.2 mm) exceeding 30 %. Consequently, data from five participants were excluded from subsequent analyses because of excessive head motion during the fMRI session. Additionally, we excluded three participants who unexpectedly took psychotropic medications immediately before the experiment and five participants who exhibited responses in one direction (all fusion or all non-fusion) for the no-tACS fMRI session. Consequently, further analyses were conducted using data from the remaining 22 participants.

### 4.5. General linear model (GLM) for fMRI analysis

Functional activation during the visual perception task was examined using the standard GLM pipeline in SPM12. The fMRI design matrix encompassing six motion parameters included stimulation and fixation conditions. Two response conditions, fusion and non-fusion, were specified based on the participant's response to the 50-ms flickering stimuli. Contrasts of interest included 'fusion – fixation', 'non-fusion – fixation', and 'fusion – non-fusion', defining the fixation condition based on the interval between the participants' response onset and the next flickering onset. In the second level analyses, one-sample *t*-tests were performed for each within-condition ('fusion – fixation' and 'non-fusion – fixation'), and paired *t*-tests were conducted for the between-condition ('fusion – non-fusion') to ascertain the statistical significance of these contrasts. To correct for multiple comparisons, a permutation-based voxel-wise nonparametric test was performed using the threshold-free cluster enhancement (TFCE) toolbox (http://dbm.neuro.uni-jena.de/tfce) (Smith and Nichols, 2009). The resulting TFCE maps were thresholded at a family-wise error (FWE) corrected $p < 0.05$ for both within-condition (fusion and non-fusion) and between-condition (fusion – non-fusion; Fig. 2 and Table S1). Based on our previous findings of sustained thalamocortical interaction during conscious perception (Min et al., 2020; Seo et al., 2022), we subsequently investigated the temporal dynamics of fMRI time series between fusion and non-fusion conditions using an event-related GLM approach with a 1-s step. Functional activation, defined based on the beta weights from the GLM, was compared using two-sided paired *t*-tests for the same contrasts of interest in the 50-ms flickering condition.

Subsequently, to investigate task-relevant thalamocortical neurodynamics, the following 12 thalamocortical regions of interest (ROIs) were selected for further analyses: the lateral geniculate nucleus (LGN), pulvinar (PUL), medial dorsal nucleus of thalamus (MD), primary visual cortex (V1), secondary visual cortex (V2), V4, dorsolateral prefrontal cortex (DLPFC), anterior insular cortex (AIC), dorsal anterior cingulate cortex (dACC), medial prefrontal cortex (mPFC), posterior cingulate cortex (PCC), and posterior parietal cortex (PPC). These ROIs included significantly activated regions during the task and crucial regions for the CEN, SN, and DMN. Three thalamic ROIs (the LGN, PUL, and MD) were anatomically defined using the Wake Forest University Pick Atlas (https://www.nitrc.org/projects/wfu_pickatlas). The remaining cortical ROIs were defined as 5-mm radius spheres centred on the peak activation of the within- and between-conditions. Each ROI plays a significant role in the CEN or DMN. For example, V1 and V2 were analysed for striate and extrastriate visual processing, respectively, and V4 was analysed as it is considered crucial for colour perception (Bartels and Zeki, 2000). Beta weights were separately averaged within these 12 ROIs and extracted for further analysis (temporal dynamics) using the region of interest extraction toolbox (http://web.mit.edu/swg/software.htm).

## Data and code availability

The data are not shared in a public repository owing to the privacy rights of the human subjects. The data and analytical tools used in the current study are available from the corresponding author upon request.

## CRediT authorship contribution statement

**Jeehye Seo:** Writing – review & editing, Visualization, Validation, Formal analysis, Data curation. **Byoung-Kyong Min:** Writing – review & editing, Writing – original draft, Visualization, Validation, Supervision, Software, Resources, Project administration, Methodology, Investigation, Funding acquisition, Formal analysis, Data curation, Conceptualization.

## Declaration of competing interest

The authors declare no competing interests.

## Data availability

Data will be made available on request.

## Acknowledgments

We thank Je-Choon Park, Je-Hyeop Lee, Jeongwook Kwon, Yukyung Kim, Sangbin Yun, and Dr. Hyoungkyu Kim for their assistance during data acquisition and figure work. This work was supported by the Convergent Technology R&D Program for Human Augmentation (grant number 2020M3C1B8081319 to B.-K.M.), which the Korean government funded through the National Research Foundation of Korea.

## Supplementary materials

Supplementary material associated with this article can be found, in the online version, at doi:10.1016/j.neuroimage.2024.120647.

## References

Alekseichuk, I., Diers, K., Paulus, W., Antal, A., 2016. Transcranial electrical stimulation of the occipital cortex during visual perception modifies the magnitude of BOLD activity: a combined tES–fMRI approach. Neuroimage 140, 110–117.
Antal, A., Bikson, M., Datta, A., Lafon, B., Dechent, P., Parra, L.C., Paulus, W., 2014. Imaging artifacts induced by electrical stimulation during conventional fMRI of the brain. Neuroimage 85, 1040–1047.
Arcaro, M.J., Pinsk, M.A., Kastner, S., 2015. The Anatomical and Functional Organization of the Human Visual Pulvinar. J. Neurosci. 35, 9848–9871.
Barron, D.S., Eickhoff, S.B., Clos, M., Fox, P.T., 2015. Human pulvinar functional organization and connectivity. Hum. Brain Mapp. 36, 2417–2431.
Bartels, A., Zeki, S., 2000. The architecture of the colour centre in the human visual brain: new results and a review. Eur. J. Neurosci. 12, 172–193.
Benjamini, Y., Hochberg, Y., 1995. Controlling the false discovery rate: a practical and powerful approach to multiple testing. J. R. Stat. Soc. 57, 289–300.
Bowmaker, J.K., Dartnall, H.J., 1980. Visual pigments of rods and cones in a human retina. J. Physiol. 298, 501–511.
Brincat, S.L., Miller, E.K., 2016. Prefrontal cortex networks shift from external to internal modes during learning. J. Neurosci. 36, 9739–9754.
Chand, G.B., Dhamala, M., 2016. Interactions among the brain default-mode, salience, and central-executive networks during perceptual decision-making of moving dots. Brain Connect. 6, 249–254.
Chang, C., Glover, G.H., 2009. Effects of model-based physiological noise correction on default mode network anti-correlations and correlations. Neuroimage 47, 1448–1459.
CIE, 1931. In: Commission Internationale de l'Éclairage Proceedings. Cambridge University Press, Cambridge, UK.
Craig, A.D., 2009. How do you feel—Now? The anterior insula and human awareness. Nat. Rev. Neurosci. 10, 59–70.
Daselaar, S.M., Porat, Y., Huijbers, W., Pennartz, C.M., 2010. Modality-specific and modality-independent components of the human imagery system. Neuroimage 52, 677–685.
Di Lollo, V., Clark, C.D., Hogben, J.H., 1988. Separating visible persistence from retinal afterimages. Percept. Psychophys. 44, 363–368.
Dosenbach, N.U., Fair, D.A., Miezin, F.M., Cohen, A.L., Wenger, K.K., Dosenbach, R.A., Fox, M.D., Snyder, A.Z., Vincent, J.L., Raichle, M.E., 2007. Distinct brain networks for adaptive and stable task control in humans. Proc. Natl. Acad. Sci. 104, 11073–11078.
Fox, M.D., Snyder, A.Z., Vincent, J.L., Corbetta, M., Van Essen, D.C., Raichle, M.E., 2005. The human brain is intrinsically organized into dynamic, anticorrelated functional networks. Proc. Natl. Acad. Sci. 102, 9673–9678.
Grinband, J., Hirsch, J., Ferrera, V.P., 2006. A neural representation of categorization uncertainty in the human brain. Neuron 49, 757–763.
Grossman, N., Bono, D., Dedic, N., Kodandaramaiah, S.B., Rudenko, A., Suk, H.-J., Cassara, A.M., Neufeld, E., Kuster, N., Tsai, L.-H., 2017. Noninvasive deep brain stimulation via temporally interfering electric fields. Cell 169, 1029–1041 e1016.
Kasten, F.H., Dowsett, J., Herrmann, C.S., 2016. Sustained aftereffect of α-tACS lasts up to 70 min after stimulation. Front. Hum. Neurosci. 10, 245.
Kasten, F.H., Herrmann, C.S., 2022. The hidden brain-state dynamics of tACS aftereffects. Neuroimage 264, 119713.
Legon, W., Ai, L., Bansal, P., Mueller, J.K., 2018. Neuromodulation with single-element transcranial focused ultrasound in human thalamus. Hum. Brain Mapp. 39, 1995–2006.
Lopes da Silva, F., 1991. Neural mechanisms underlying brain waves: from neural membranes to networks. Electroencephalogr. Clin. Neurophysiol. 79, 81–93.
Menon, V., Uddin, L.Q., 2010. Saliency, switching, attention and control: a network model of insula function. Brain Struct. Funct. 214, 655–667.
Miller, E.K., Lundqvist, M., Bastos, A.M., 2018. Working Memory 2.0. Neuron 100, 463–475.
Min, B.-K., 2010. A thalamic reticular networking model of consciousness. Theor. Biol. Med. Model 7, 10.
Min, B.-K., Kim, H.-S., Ko, W., Ahn, M.-H., Suk, H.-I., Pantazis, D., Knight, R.T., 2021. Electrophysiological decoding of spatial and color processing in human prefrontal cortex. Neuroimage 237, 118165.
Min, B.K., Kim, H.S., Pinotsis, D.A., Pantazis, D., 2020. Thalamocortical inhibitory dynamics support conscious perception. Neuroimage 220, 117066.
Nekovarova, T., Fajnerova, I., Horacek, J., Spaniel, F., 2014. Bridging disparate symptoms of schizophrenia: a triple network dysfunction theory. Front. Behav. Neurosci. 8, 171.
Peters, S.K., Dunlop, K., Downar, J., 2016. Cortico-striatal-thalamic loop circuits of the salience network: a central pathway in psychiatric disease and treatment. Front. Syst. Neurosci. 10, 104.
Ramírez-Barrantes, R., Arancibia, M., Stojanova, J., Aspé-Sánchez, M., Córdova, C., Henríquez-Ch, R.A., 2019. Default Mode Network, Meditation, and Age-Associated Brain Changes: what Can We Learn from the Impact of Mental Training on Well-Being as a Psychotherapeutic Approach? Neural Plast. 2019, 7067592.
Seeley, W.W., Menon, V., Schatzberg, A.F., Keller, J., Glover, G.H., Kenna, H., Reiss, A.L., Greicius, M.D., 2007. Dissociable intrinsic connectivity networks for salience processing and executive control. J. Neurosci. 27, 2349–2356.
Seo, J., Kim, D.-J., Choi, S.-H., Kim, H., Min, B.-K., 2022. The thalamocortical inhibitory network controls human conscious perception. Neuroimage 264, 119748.
Sherman, S.M., 2016. Thalamus plays a central role in ongoing cortical functioning. Nat. Neurosci. 19, 533–541.
Shine, J.M., Muller, A.J., O'Callaghan, C., Hornberger, M., Halliday, G.M., Lewis, S.J.G., 2015. Abnormal connectivity between the default mode and the visual system underlies the manifestation of visual hallucinations in Parkinson's disease: a task-based fMRI study. npj Parkinson's Dis. 1, 15003.
Shu, Y.S., McCormick, D.A., 2002. Inhibitory interactions between ferret thalamic reticular neurons. J. Neurophysiol. 87, 2571–2576.
Smallwood, J., Turnbull, A., Wang, H.T., Ho, N.S.P., Poerio, G.L., Karapanagiotidis, T., Konu, D., Mckeown, B., Zhang, M.C., Murphy, C., Vatansever, D., Bzdok, D., Konishi, M., Leech, R., Seli, P., Schooler, J.W., Bernhardt, B., Margulies, D.S., Jefferies, E., 2021. The neural correlates of ongoing conscious thought. iScience 24.
Smith, S.M., Nichols, T.E., 2009. Threshold-free cluster enhancement: addressing problems of smoothing, threshold dependence and localisation in cluster inference. Neuroimage 44, 83–98.
Sormaz, M., Murphy, C., Wang, H.T., Hymers, M., Karapanagiotidis, T., Poerio, G., Margulies, D.S., Jefferies, E., Smallwood, J., 2018. Default mode network can support the level of detail in experience during active task states. Proc. Natl. Acad. Sci. U.S.A. 115, 9318–9323.
Sridharan, D., Levitin, D.J., Menon, V., 2008. A critical role for the right fronto-insular cortex in switching between central-executive and default-mode networks. Proc. Natl. Acad. Sci. 105, 12569–12574.
Stawarczyk, D., Majerus, S., Maquet, P., D'Argembeau, A., 2011. Neural Correlates of Ongoing Conscious Experience: both Task-Unrelatedness and Stimulus-Independence Are Related to Default Network Activity. PLoS ONE 6.
Thielscher, A., Antunes, A., Saturnino, G.B., 2015. Field modeling for transcranial magnetic stimulation: a useful tool to understand the physiological effects of TMS?. In: 2015 37th annual international conference of the IEEE engineering in medicine and biology society (EMBC). IEEE, pp. 222–225.
Uddin, L.Q., Menon, V., 2009. The anterior insula in autism: under-connected and under-examined. Neurosci. Biobehav. Rev. 33, 1198–1203.
Ullsperger, M., Harsay, H.A., Wessel, J.R., Ridderinkhof, K.R., 2010. Conscious perception of errors and its relation to the anterior insula. Brain Struct. Funct. 214, 629–643.
Vosskuhl, J., Huster, R.J., Herrmann, C.S., 2016. BOLD signal effects of transcranial alternating current stimulation (tACS) in the alpha range: a concurrent tACS–fMRI study. Neuroimage 140, 118–125.
Zhang, L., Luo, L., Zhou, Z., Xu, K., Zhang, L., Liu, X., Tan, X., Zhang, J., Ye, X., Gao, J., 2018a. Functional connectivity of anterior insula predicts recovery of patients with disorders of consciousness. Front. Neurol. 9, 1024.
Zhang, Z., Zhang, D., Wang, Z., Li, J., Lin, Y., Chang, S., Huang, R., Liu, M., 2018b. Intrinsic neural linkage between primary visual area and default mode network in human brain: evidence from visual mental imagery. Neuroscience 379, 13–21.